The Kramers Kronig coherent receiver

ANTONIO MECOZZI[1,*], **CRISTIAN ANTONELLI**[1], **AND MARK SHTAIF**[2]

[1] *Department of Physical and Chemical Sciences, University of L'Aquila, L'Aquila 67100, Italy.*
[2] *Department of Physical Electronics, Tel Aviv University, Tel Aviv 69978, Israel.*
[*] *Corresponding author: antonio.mecozzi@univaq.it*

Compiled June 21, 2016

The interest for short-reach links of the kind needed for inter-data center communications has fueled in recent years the search for transmission schemes that are simultaneously highly performing and cost-effective. In this work we propose a direct-detection coherent receiver which combines the advantages of coherent transmission and the cost-effectiveness of direct detection. The working principle of the proposed receiver is based on the famous Kramers-Kronig (KK) relations, and its implementation requires transmitting a continuous-wave signal at one edge of the information-carrying signal spectrum. The KK receiver scheme allows digital post-compensation of linear propagation impairments and, as compared to other existing solutions, is more efficient in terms of spectral occupancy and energy consumption.

OCIS codes: *(060.2330) Fiber optics communications; (060.4080) Modulation; (060.2840) Heterodyne; (100.5070) Phase retrieval.*

http://dx.doi.org/10.1364/optica.XX.XXXXXX

1. INTRODUCTION

Coherent optical transmission schemes are optimal from the standpoint of spectral efficiency as they allow the encoding of information in both quadratures and polarizations of the electric field. However, while they constitute the solution of choice for medium-to-long reach applications, the cost of a coherent receiver is a major obstacle in the case of short-reach links, whose role in many areas of applications is becoming increasingly important. Indeed, coherent receivers used today are based on the intradyne scheme, which requires two optical hybrids and four pairs of balanced photodiodes,making its overall cost unacceptably high for short links, such as those intended for inter-data center communications. In recent years, the need for low-cost solutions has lead to a number of simpler, direct-detection based, transmission schemes [1]. Most common is the pulse-amplitude modulation (PAM) scheme, which relies on the transmission of pulses of several amplitudes. Another popular approach is that of direct-detection orthogonal frequency-division multiplexing (OFDM) [2] (also referred to as digital multi-tone (DMT)), where the OFDM tones are constrained to be symmetric with respect to the center frequency (for the signal to be real-valued), and where a bias is introduced so as to prevent signal negativity. A shortcoming of the above two methods is that they are not tolerant to linear propagation effects, primarily chromatic and polarization-mode dispersion. In order to resolve this issue, Lowery and Armstrong proposed the self coherent heterodyne scheme [3, 4], where a frequency offset local oscillator (LO) is launched into the system together with the signal, thereby allowing full reconstruction of the complex-valued field by means of direct detection. This approach allows the elimination of linear propagation impairments by using standard digital signal processing (DSP), but it also involves two important disadvantages. Firstly, the power budget becomes less favorable, as a notable fraction of the launched power needs to be allocated to the local oscillator. Secondly, in order to avoid interference, the local oscillator must be separated from the data carrying signal by a frequency gap that is at least as large as the signal's bandwidth, thereby resulting in a reduction of the spectral efficiency by at least a factor of two. A scheme that avoids the frequency gap was proposed by Schuster *et al.* [5]. However, the higher spectral efficiency is achieved at the expense of flexibility, because this scheme, unlike the self coherent heterodyne scheme, does not allow digital compensation of linear propagation impairments, and is thereby mainly suited for short range OFDM-based transmission systems. More recently, another single-sideband modulation/direct-detection scheme, which in principle is capable of full field reconstruction, has been reported in [6].

In this paper we introduce a new communication scheme, to which we refer as the self-coherent Kramers-Kronig (KK) method.[1] Our scheme consists of the same optical building blocks as the ones used in the scheme of Lowery and Armstrong [3, 4], but, similarly to [5] and [6], it eliminates the need for a frequency gap between the local oscillator and the signal and hence increases the spectral efficiency by a factor of two in comparison with that scheme. The extraction of the received complex-valued

[1] Towards the completion of this paper, we discovered that a similar scheme was proposed in [7]. That scheme was presented in the context of analog radio systems and it did not contain the features that characterize fiber-optic transmission, and which are discussed in this paper.

signal from the photocurrent is performed digitally while taking advantage of the Kramers-Kronig (KK) relations between the phase and amplitude of the field impinging upon the photodiode, thereby justifying our choice for the scheme's name. The KK relations are somewhat ubiquitous, as they emerge in various areas of physics and engineering [8–12]. Their applicability in the context of direct-detection coherent receivers follows from a simple property of minimum phase signals, as discussed in [13, 14]. Unlike the method of [5], the proposed scheme allows the full reconstruction of the complex envelope of the optical filed impinging upon the receiver, and hence it is compatible with DSP-based digital compensation of propagation-induced linear impairments. The gain in spectral efficiency comes at the expense of a somewhat more stringent requirement on the power of the transmitted local oscillator tone in comparison with the self-heterodyne scheme. Nonetheless, as we show in what follows, in practical scenarios this power requirement can be considerably relaxed. We show that the proposed KK-scheme is optimal in terms of information capacity with respect to the class of band-limited systems whose receivers are constrained to detect only the signal's intensity. Finally, we note that the methods that we discuss here are of relevance to the broader topic of phase reconstruction that has been attracting significant interest in many areas of optics [15].

2. MINIMUM PHASE SIGNALS

The communications scheme presented in this paper relies on identifying a condition that ensures that the received signal is minimum phase, in which case its phase can be uniquely extracted from its intensity. We denote by $s(t)$ a complex data-carrying signal whose spectrum is contained between $-B/2$ and $B/2$, and consider a single sideband signal of the form

$$h(t) = A + s(t)\exp(-i\pi Bt)\,, \tag{1}$$

where A is a constant. As described in [14], the Nyquist stability criterion [16] can be used to prove that $h(t)$ is a minimum phase signal if and only if its time trajectory in the complex plain does not encircle the origin. The illustration in Fig. 1 shows that this condition is satisfied when $|A|$ is sufficiently large. Evidently, the condition $|A| > |s(t)|$ is sufficient for guaranteeing the minimum phase property, as was originally reported in [13], and as we also demonstrate in the appendix. When $h(t)$ is a minimum-phase signal, its phase $\phi(t)$ and absolute value $|h(t)|$ are uniquely related by the Hilbert transform,

$$\phi(t) = \frac{1}{\pi}\text{p.v.}\int_{-\infty}^{\infty} dt' \frac{\log[|h(t')|]}{t-t'}, \tag{2}$$

where p.v. stands for *principal value*. Equation (2) is one of the two Kramers-Kronig relations existing between ϕ and $\log[|h|]$, and it is most conveniently implemented in the frequency domain, where it assumes the form

$$\tilde{\phi}(\omega) = i\,\text{sign}(\omega)\mathcal{F}\{\log[|h(t)|]\}\,, \tag{3}$$

where $\text{sign}(\omega)$ is the sign function, which is equal to 1 for $\omega > 0$, to 0 for $\omega = 0$, and to -1 for $\omega < 0$, and where $\mathcal{F}$ denotes a Fourier transform. It should be noted that the phase reconstruction is exact up to a constant phase offset. This can be seen most easily from Eq. (3), where the zero-frequency component of $\tilde{\phi}(\omega)$ is set to zero by the sign function.

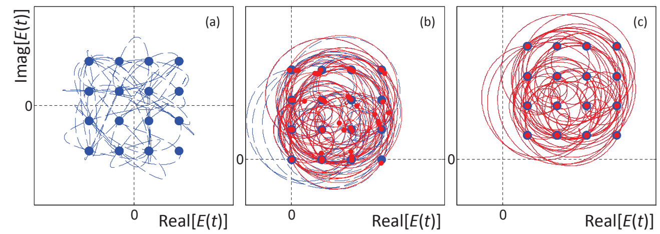

Fig. 1. (a) The time trajectory of a 16 QAM modulated signal $s(t)$ of bandwidth B in the complex plane. (b) The time trajectory of the single-sideband signal $A + s(t)\exp(-i\pi Bt)$ (blue dashed) and of the signal reconstructed from its intensity (red solid). We set the phase of A to 45° for the convenience of illustration. The blue and red dots are the original and reconstructed symbols, respectively. The quality of the reconstruction is poor owing to the fact that the original signal encircles the origin multiple times. (c) Same as (b), but with a larger value of $|A|$. Here the trajectory of the original signal does not encircle the origin, and the reconstruction is perfect.

3. THE KK SCHEME

We proceed to describing the field reconstruction procedure performed by the KK receiver, where we assume for simplicity a scalar description of the field, and ignore, for the time being, fiber propagation effects. The treatment of vector fields follows trivially from applying the scalar description individually to each of the two orthogonal polarization components.

We denote the complex envelope of the incoming electric field by $E_s(t)$, which is assumed to be contained within a finite optical bandwidth denoted by B. The local oscillator is assumed to be a continuous wave (CW) signal whose amplitude is E_0 and whose frequency coincides with the left edge of the information-carrying signal spectrum. We assume that E_0 is real-valued and positive, which is equivalent to referring all phase values to that of the local oscillator. The complex envelope of the field impinging upon the photodiode is thus $E(t) = E_s(t) + E_0\exp(i\pi Bt)$. Provided that the local oscillator amplitude is chosen such that $E_0 > |E_s(t)|$ for all t, the signal $E(t)\exp(-i\pi Bt) = E_0 + E_s(t)\exp(-i\pi Bt)$ is minimum phase, according to the above theorem. The photocurrent I produced by the photodiode is proportional to the field intensity $I = |E(t)|^2$, where we have set the proportionality coefficient to 1, for the sake of simplicity. Hence, using Eqs. (2) and (3), the signal $E_s(t)$ can be reconstructed as follows

$$E_s(t) = \left\{\sqrt{I(t)}\exp[i\phi_E(t)] - E_0\right\}\exp(i\pi Bt)\,, \tag{4}$$

$$\phi_E(t) = \frac{1}{2\pi}\text{p.v.}\int_{-\infty}^{\infty} dt' \frac{\log[I(t')]}{t-t'}. \tag{5}$$

Note that the cancellation of the average phase is immaterial if $E_s(t)$ is isotropically distributed in the complex plane, which is the case with all relevant complex (I/Q) modulation formats.

A possible issue with the signal reconstruction described above is that the logarithm appearing in Eq. (5) introduces spectral broadening which necessitates digital up-sampling of the received photocurrent. An alternative signal reconstruction approach that resolves this issue makes use of the fact that the frequency shifted signal $E_s'(t) = E_s(t)\exp(-i\pi Bt)$ has real and

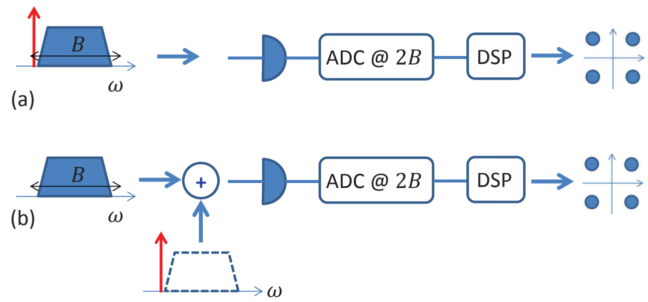

Fig. 2. a) The KK receiver scheme: the transmitted waveform, which consists of a modulated signal of bandwidth B and a CW field at the left edge of the signal spectrum, is directly detected, then sampled at the sampling rate of $2B$. The digital samples are finally processed for chromatic dispersion compensation and extraction of the transmitted symbols. (b) An alternative version of the KK scheme. In this case the CW field at the left edge of the modulated signal spectrum is added at the receiver using a frequency selective coupler.

imaginary parts $E'_{s,r}(t)$ and $E'_{s,i}(t)$ satisfying the KK relations,

$$E'_{s,i}(t) = \frac{1}{\pi}\text{p.v.}\int_{-\infty}^{\infty} \mathrm{d}t' \frac{E'_{s,r}(t')}{t-t'}. \tag{6}$$

Using $I(t) = |E_0 + E'_s(t)|^2$ one obtains the equality

$$I(t) = E_0^2 + E'^2_{s,r}(t) + E'^2_{s,i}(t) + 2E_0 E'_{s,r}(t). \tag{7}$$

Once $E'_{s,i}(t)$ is replaced by its expression given by Eq. (6), Eq. (7) becomes an integral equation that, being equivalent to Eqs. (4) and (5), has a unique solution if the condition in [14] is satisfied (or when $E_0 > |E_s(t)|$ for all t, as in [13]). This solution can be obtained by means of the procedure described in what follows, and which avoids the need of significant up-sampling. Equation (7) can be formally solved for $E'_{s,r}(t)$ with the result

$$E'_{s,r}(t) = \sqrt{I(t) - E'^2_{s,i}(t)} - E_0, \tag{8}$$

where we have taken the positive determination of the square root because it is the only one consistent with the minimum-phase condition. Equation (8) can be solved by iterations, where in the first step one solves for $E'_{s,r}(t)$ while setting $E'_{s,i}(t) = 0$ on the right hand side of (8). The resulting $E'_{s,r}(t)$ is then filtered using a square filter of bandwidth B, and used to extract the next iteration of $E'_{s,i}(t)$ through Eq. (6). The procedure is then repeated until the values of $E'_{s,r}(t)$ and $E'_{s,i}(t)$ stabilize. For the purpose of demonstrating the KK scheme we assume in this paper that the oversampling of the photocurrent is not an issue and hence in what follows we apply the procedure represented in Eqs. (2)–(5).

The implementation of the KK transceiver is plotted in Fig. 2a. Figure 2b shows an alternative implementation, where the local oscillator is added to the information carrying signal at the receiver using a frequency-selective coupler to avoid signal and local oscillator loss. This implementation accommodates polarization multiplexing, eliminates the need for an optical hybrid at the receiver, and requires the use of a single photodiode. However, it is more costly as it requires a local oscillator laser, and hence it is less suitable for short-reach links. Moreover, in this implementation the complexity of the receiver hardware is comparable to that of the balanced heterodyne receiver, while the complexity of the post-detection processing is somewhat higher. For this reason in what follows we restrict ourselves on the first implementation of the KK scheme, targeting short-reach transmission systems.

Since the bandwidth of the photocurrent I is twice larger than the bandwidth of the information carrying optical signal, the minimum sampling rate that is required according to Shannon-Nyquist sampling theorem is $2B$. The doubling of the bandwidth is consistent with the fact that the information that was previously encoded in a complex-valued signal, is transferred by square-law detection into a real-valued signal without loss. The photocurrent samples are digitally up-sampled and then the natural logarithm operation is performed. The up-sampling is required so as to accommodate the increase in bandwidth caused by the logarithm operation. A method for avoiding the need for up-sampling was discussed in the previous section. Subsequently, a Hilbert transform is applied so as to obtain the phase ϕ_E and the complex signal $E_s(t)$, according to Eqs. (4) and (5). At this stage the signal $E_s(t)$ can be down-sampled to the original sampling rate. The subsequent digital processing of the received signal is identical to the one that is found in standard coherent receivers, and is not detailed in the figure.

4. THE OPTIMALITY OF THE KK SCHEME

An important attribute of the KK-scheme is that it is optimal in terms of information capacity with respect to the entire class of band-limited systems that are constrained to work with receivers that are only capable of detecting the signal's intensity. This optimality is demonstrated by two arguments. The first is that all minimum phase signals can be expressed in the form of Eq. (1), and communicated using the KK-configuration. The second is that of all signals with a given intensity waveform in the time domain, the minimum phase signal is contained in the smallest bandwidth. The latter argument follows from the minimum-energy-delay property of minimum phase signals discussed in [17], with the only difference being that the time and frequency variables are interchanged.[2] The formal statement of this property is that the quantity $\int_{\omega_0}^{\infty}|\tilde{E}(\omega)|^2\mathrm{d}\omega$ is minimized when $\tilde{E}(\omega)$ is the Fourier transform of a minimum phase signal.[3]

5. NUMERICAL VALIDATION OF THE KK RECEIVER

We start by providing a numerical proof-of-concept of the KK receiver scheme. To that end we consider the case in which the signal impinging upon the receiver is produced by filtering white Gaussian noise with a square optical filter of bandwidth B. Since Gaussian noise is characterized by the largest entropy that can be carried by signals of the same bandwidth, it seems natural to use it for validating the KK receiver concept.

Figure 3 shows the absolute values of the original and the reconstructed waveforms by solid and dot-dashed lines, respectively (a similar picture corresponds to the real or imaginary

[2]Recall that, contrary to [17] and to most of the existing literature, we are considering signals that are 'causal' in the frequency domain, i.e. such that vanish for $\omega < 0$.

[3]In order to see why the minimum energy-delay property implies that of all signals with the same intensity profile the minimum phase signal is contained within the smallest bandwidth, consider the following situation. Assume that $E(t)$ is a minimum phase signal, whose spectrum $|\tilde{E}(\omega)|^2$ is contained in the bandwidth B, but exceeds any bandwidth $B' < B$. If there were a signal $E'(t)$ such that $|E'(t)|^2 = |E(t)|^2$, with a spectrum $|\tilde{E}(\omega)|^2$ that is contained in $B' < B$, then we would have $\int_{\omega_0}^{\infty}|\tilde{E}(\omega)|^2\mathrm{d}\omega > \int_{\omega_0}^{\infty}|\tilde{E}'(\omega)|^2\mathrm{d}\omega = 0$ for every $\omega_0 \in (B', B)$, contrary to the minimum energy-delay property.

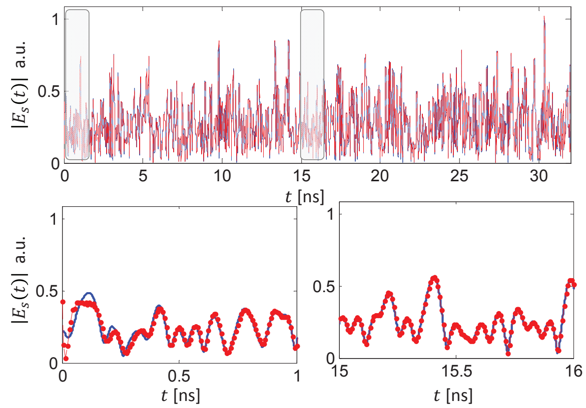

Fig. 3. The top panel shows the absolute values of the original (solid blue) and reconstructed (dashed red) waveforms. The bottom left and right panels zoom into the beginning and the center of the frame, respectively.

parts). The computation was performed with $B = 32$GHz, using a time window $T = 1024/B$. The signal samples used to perform the Hilbert transform were taken at a rate of $2B$. The signal used in the simulation was generated as a complex-valued circular Gaussian waveform with a flat-top spectrum of width $B = 32$GHz, which was normalized such that its largest absolute value within the simulated time window was $0.99E_0$. The top panel shows the signal intensity within the entire simulated time window, whereas the bottom panels zoom into the waveform in two distinct intervals. In the left panel we show the beginning of the frame, where the edge effect of the Hilbert transform is visible. The waveform reconstruction error is large initially, but then it reduces as the distance from the beginning of the frame increases. The waveform in the right panel is taken from the middle of the frame, where the edge effect is absent, and the quality of the reconstruction is excellent. As can be seen in the figure, the duration of the edge effect is of the order of 0.5ns, which is equivalent to $\sim 16/B$. The edges in the beginning and in the end of the processed frame will have to be discarded in a practical implementation of the KK receiver. As is discussed in what follows, a similar situation, where the edges of the processed frame need to be discarded, characterizes the digital compensation of chromatic dispersion.

6. LINEAR TRANSMISSION PERFORMANCE

We now switch to demonstrating the implementation of the KK transceiver in the context of a digital communication system transmitting QAM signals. We focus first on the linear regime of operation, where the effect of the fiber nonlinearity is negligible.

Figure 4 refers to the back-to-back configuration. The panels show the received constellations for single-channel 16-QAM signaling, where a raised cosine fundamental waveform with 0.05 roll-off factor was assumed. Since this figure was plotted in the regime of linear transmission, and in the absence of noise, the displayed results are not affected by the baudrate. The various panels correspond to different settings of the local oscillator power $P_{\text{LO}} = E_0^2$. In the leftmost panel the local oscillator power was set to 1.1 times the maximum value of the information carrying signal power, corresponding to about 11dB above the average signal power, and the received constellation was indeed perfect (the edge-effect seen in Fig. 3 was taken care of by

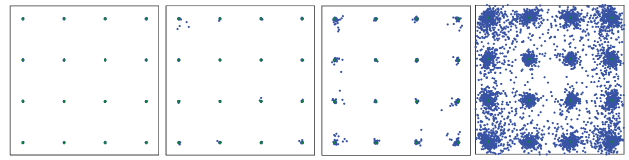

Fig. 4. Received constellations in the back-to-back configuration. In the leftmost panel the local oscillator power was set to 1.1 times the maximum value of the information carrying signal power – corresponding to about 11dB above the average signal power. In this case the minimum-phase condition [13, 14] is rigorously fulfilled. In the second, third and fourth panels, the local oscillator power level was reduced by 3, 5 and 8dB, respectively, while not modifying the signal.

discarding the symbols at the edges of the simulation time window). In the remaining three panels, the local oscillator power level was reduced to 8, 6 and 3dB above the average channel power. The figure shows that the received constellation quality deteriorates as the power of the local oscillator is reduced. The scattering of the constellation points is caused by the fact that the instantaneous power of the information carrying signal occasionally exceeds the local oscillator power to an extent that it violates the minimum-phase condition required for signal reconstruction [13].

Practical considerations suggest that one should pick the lowest local oscillator power for which the reconstruction noise shown in Fig. 4 is sufficiently small to allow reliable detection. Indeed large values of the local oscillator power would deteriorate the system's power efficiency and, as we show in the next section, reduce its tolerance to propagation-induced nonlinear distortions.

In Fig. 5 we characterize the penalty introduced by a non-compliant local oscillator power in the presence of amplification noise. Plotted in the figure is the BER as a function of OSNR for a 24Gbaud 16 QAM modulated signal, for a range of LO powers. Empty markers show the results obtained in the back-to-back configuration, whereas filled markers refer to the case of *linear* transmission through a 100km single-mode fiber link. In the latter case chromatic dispersion was compensated electronically at the receiver, after signal reconstruction. In all simulations the information-carrying signal consisted of a pseudo-random sequence of 2^{14} symbols. Prior to reception, amplification noise was added to the signal and then a 12th order super-Gaussian optical filter with a 3dB bandwidth of 40GHz was applied. The figure confirms the benefit of increasing the LO power: at low levels the BER saturates for increasing OSNR, owing to the errors caused by imperfect signal reconstruction. This saturation tends to disappear when the LO power is sufficiently large. The difference between the back-to-back results and the results obtained with SMF transmission shows that electronic CD compensation implies an OSNR penalty, as well as an increase in the smallest achievable BER. The reason for this penalty is in the larger peak-to-average power ratio (PAPR) of the CD-impaired information-carrying signal, as compared to the PAPR of the launched signal. The OSNR penalty could in principle be avoided either by pre-compensating the modulated signal, or by implementing *optical* CD compensation at the receiver, although this would imply an obvious complication of the transceiver structure.

The results of Fig. 5 indicate that for OSNR values higher than 20dB, pre-FEC BERs lower than 10^{-2} can be achieved with

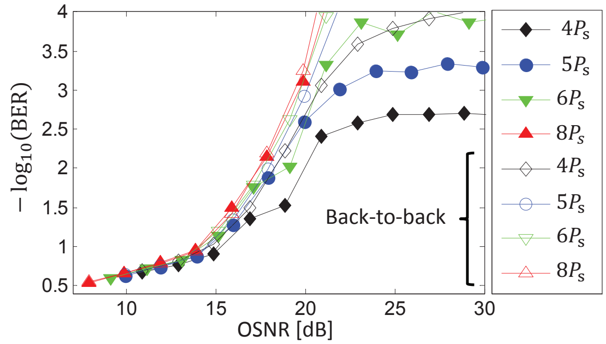

Fig. 5. BER versus OSNR for a 24Gbaud 16 QAM modulated signal. Each curve was obtained by setting the power of the local oscillator to the value shown in the legend. Empty markers refer to the back-to-back configuration, while filled markers were obtained for a 100km single-span link, where CD was compensated electronically at the receiver after signal reconstruction.

a local oscillator power exceeding the average channel power by about 7 dB (implying that the total transmitted power increases by 7.8dB relative to coherent transmission). This makes the KK scheme considerably more power efficient than the scheme proposed recently in [6], but less efficient than IMDD and self-heterodyne [3, 4]. On the other hand, it should be stressed that the KK scheme is twice more spectrally efficient than IMDD[4] and the self-heterodyne scheme. A detailed comparison with other known direct-detection schemes in terms of spectral efficiency, power efficiency, and amenability to digital dispersion compensation, is shown in Table 1. To facilitate the comparison of spectral efficiencies, we express the optical bandwidth in terms of R, which is the lowest sampling rate that allows reconstruction of the detected photocurrent.[5] As can be seen from the table, the KK scheme provides an attractive combinations of properties.

7. NONLINEAR TRANSMISSION PERFORMANCE

In this section we investigate the limitations imposed by the fiber nonlinearity to the implementation of the KK transceiver in coherent transmission systems of the kind considered in the previous section. The main results of this investigation are presented in Fig. 6, which was obtained for a DWDM system with five 16 QAM channels at 24 Gbaud. The channel spacing was set to 40GHz. The BER of the channel of interest is plotted in Fig. 6 as a function of the total transmit power, which is the sum of the channel power and the local oscillator power. The left panel and the right panel refer to a one-span and two-span system, respectively, where in both cases a standard SMF was assumed. Here too the various curves correspond to different values of the LO power, and CD was compensated digitally after signal reconstruction.

[4]The lower spectral efficiency of IMDD follows from the fact that with intensity modulation no information is encoded into the optical phase. This makes IMDD inferior even to single-quadrature modulation, where positive and negative amplitude values can be used.

[5] The rate R is in general different from the actual sampling rate. For instance, in the experimental implementation of the scheme of [3] presented in [4], the sampled photocurrent includes the contribution of the spurious signal-signal beat, which is filtered out in the digital domain, so that the minimum sampling rate is $2R$. In addition, in most practical implementations, the sampling rate is equal to twice the symbol rate, and hence it is higher than R.

Table 1. Comparison between various schemes in terms of optical bandwidth, suitability for digital compensation of linear impairments, and power efficiency. The symbol R represents the bandwidth of the detected photocurrent, which is also the lowest acceptable sampling rate. The ratio P_{LO}/P_s ranges from 10 to 20 in [5], and is of the order of 30 in [6]. This ratio reduces to values ranging from 4 to 8 in the case of the KK scheme.

	Optical bandwidth	Digital compensation	P_{LO}/P_s
IMDD	R	not possible	N/A
Self heterodyne [3]	R	possible	~ 1
Ref. [5]	$R/2$	not possible	$\gg 1$
Ref. [6]	$R/2$	possible	$\gg 1$
KK	$R/2$	possible	> 1

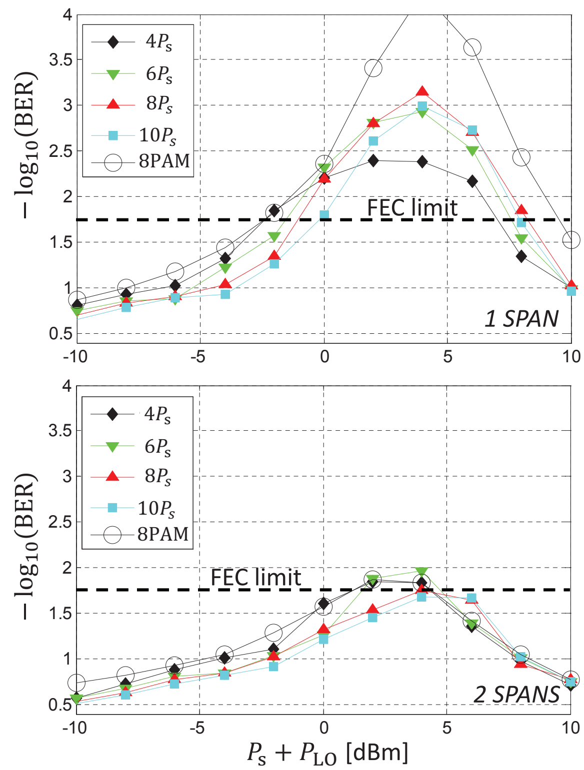

Fig. 6. BER versus total transmit power for the channel of interest of a DWDM system with five transmitted channels. The filled markers were obtained for 16 QAM modulation based on the use of the KK scheme with various levels of the local oscillator power; the empty circles show the results obtained for 8PAM modulation. In the KK scheme CD was compensated digitally after signal reconstruction, whereas in the case of 8PAM CD was compensated optically. Top and bottom panels differ by the number of spans.

As can be seen in the figure, the FEC threshold of 1.5×10^{-2} is exceeded for a broad range of power levels. As expected, the BER improves with the launched power, until it reaches an optimal values, after which it increases as a result of growing nonlinear distortions. The effect of the local oscillator power is dual. On the one hand it improves the compliance with the minimum-phase condition, which is beneficial for the BER. But on the other hand, it enhances the nonlinear distortion, whose effect on the BER is adverse. For this reason, the dependence of the peak BER on the LO power is not monotonic. In the example of Fig. 6, the peak BER reduces by increasing the LO power from 6dB ($P_{\rm LO} = 4P_{\rm ch}$) to 9dB, and then it increases when the LO power is raised beyond nine times the average power of the data-carrying signal. In parallel, the range of channel powers for which the FEC requirement is satisfied shrinks fairly monotonically with increasing LO power.

For comparison we show in the same figure the BER of an 8PAM system operated at the baudrate of 32Gbaud, so as to provide the same throughput. In this case the channel spacing was set to 50GHz, and optical CD compensation was implemented at the receiver. The fundamental waveform used was the same as in the case of 16 QAM modulation and eight equally spaced *amplitude* (not intensity) levels were used to encode the information. The figure shows that 8PAM modulation (at least the idealized implementation that we simulated in this work) over-performs 16 QAM in terms of optimum BER in the single-span configuration, but no substantial difference is visible in the two-span configuration. We remind that the reduced performance of 16 QAM comes with a smaller spectral occupancy.

8. CONCLUSIONS

We proposed and demonstrated numerically a direct-detection receiver scheme for coherent communications. The principle underpinning the proposed receiver is based on the famous Kramers-Kronig relations, while its implementation requires transmitting a CW signal at one edge of the information-carrying signal. The KK receiver allows the full reconstruction of received complex signal from the detected photocurrent, and hence the digital compensation of chromatic dispersion. We showed that KK receiver favorably compares to existing schemes in terms of power consumption and is optimal in terms of spectral efficiency.

APPENDIX: PROOF OF THE SUFFICIENT MINIMUM-PHASE CONDITION

The necessary and sufficient condition that characterizes minimum phase signals follows from the Nyquist criterion, as described in [14]. A sufficient condition was derived in [13], and we prove it here in a way that relates more directly to the set-up considered in this paper.

In the case of a single-sideband signal $u(t) = u_r(t) + iu_i(t)$, the real and imaginary parts $u_r(t)$ and $u_i(t)$ are related through the Kramers-Kronig relations. A straightforward way to see this is based on expressing its Fourier transform $\tilde{u}(\omega)$ as $\tilde{u}(\omega) = (1/2)[1 + \mathrm{sign}(\omega)]\tilde{u}(\omega)$, which follows from the single-sideband condition $\tilde{u}(\omega) = 0$ for all $\omega < 0$. Using integration by parts together with the fact that the inverse Fourier transform of $\mathrm{sign}(\omega)$ is $-i/(\pi t)$, it follows that $u(t) = u(t)/2 + i\,\mathrm{p.v.} \int_{-\infty}^{\infty} \mathrm{d}t' u(t')/[2\pi(t-t')]$, that is $u(t) = i\,\mathrm{p.v.} \int \mathrm{d}t' u(t')/[\pi(t-t')]$, from which the famous KK relations [8, 9] follow

$$u_r(t) = -\mathrm{p.v.} \int_{-\infty}^{\infty} \frac{u_i(t')\mathrm{d}t'}{\pi(t-t')}, \quad u_i(t) = \mathrm{p.v.} \int_{-\infty}^{\infty} \frac{u_r(t')\mathrm{d}t'}{\pi(t-t')}. \quad \textbf{(9)}$$

Let us now define $1 + u(t) = |1 + u(t)| \exp[i\varphi(t)]$ and consider the function $U(t) = \log[1 + u(t)] = \log|1 + u(t)| + i\varphi(t)$. The terms $|U(t)| = \log|1 + u(t)|$ and $\varphi(t)$ are the real and imaginary parts of the new function $U(t)$. In what follows we demonstrate that the condition $|u(t)| < 1$ guarantees that $U(t)$ is single sideband, and hence $|U(t)|$ and $\varphi(t)$ are also related through KK relations identical to (9).

With the condition $|u(t)| < 1$ for all t, we may expand $U(t) = \log[1 + u(t)] = \sum_{n=1}^{\infty} (-1)^{n+1} u^n(t)/n$. Since the spectrum of $u^n(t)$ is the n-th order autoconvolution of $\tilde{u}(\omega)$, it is zero for $\omega < 0$ and hence the spectrum of $U(t)$ is single sideband (i.e it is zero for all $\omega < 0$), thereby implying the equality

$$\varphi(t) = \mathrm{p.v.} \int_{-\infty}^{\infty} \mathrm{d}t' \frac{\log|1 + u(t')|^2}{2\pi(t-t')}. \quad \textbf{(10)}$$

Defining $E_s(t) = E_0 u(t)$, where E_0 is a real positive quantity, and using the fact that $\mathrm{p.v.} \int \mathrm{d}t' \log(E_0^2)/[2\pi(t-t')] = 0$, we obtain

$$\phi_E(t) = \mathrm{p.v.} \int_{-\infty}^{\infty} \mathrm{d}t' \frac{\log|E_0 + E_s(t)|^2}{2\pi(t-t')}, \quad \textbf{(11)}$$

whereby substituting $I(t) = |E_0 + E_s(t)|^2$, Eq. (5) is obtained. Equation (11) states that $\phi_E(t)$ is the Hilbert transform of $\log[I(t)]$.

ACKOWLEDGEMENT

Authors acknowledge valuable consultations with Peter J. Winzer, Robert Killey, and Shalva Ben-Ezra. A. Mecozzi and C. Antonelli also acknowledge financial support from the Italian Government under Cipe resolution n. 135 (Dec. 21, 2012), project INnovating City Planning through Information and Communication Technologies (INCIPICT).

REFERENCES

1. S. Randel, F. Breyer, S.C.J. Lee, and J.W. Walewski, "Advanced Modulation Schemes for Short-Range Optical Communications," IEEE J. Sel. Topics Quantum Electron. **16**, 1280–1289 (2010).
2. T. Takahara, T. Tanaka, M. Nishihara, Y. Kai, L. Li, Z. Tao, and J. Rasmussen, "Discrete Multi-Tone for 100 Gb/s Optical Access Networks," in Optical Fiber Communication Conference, OSA Technical Digest (online) (Optical Society of America, 2014), paper M2I.1.
3. A.J. Lowery and J. Armstrong, "Orthogonal-frequency-division multiplexing for dispersion compensation of long-haul optical systems," Opt. Express **14**, 2079–2084 (2006).
4. B.J.C. Schmidt, A.J. Lowery, and J. Armstrong, "Experimental Demonstrations of Electronic Dispersion Compensation for Long-Haul Transmission Using Direct-Detection Optical OFDM," J. Lightwave Technol. **26**, 196–203 (2008).
5. M. Schuster, S. Randel, C.A. Bunge, S.C.J. Lee, F. Breyer, B. Spinnler, and K. Petermann, "Spectrally Efficient Compatible Single-Sideband Modulation for OFDM Transmission With Direct Detection," IEEE Photon. Technol. Letters **20**, 670–672 (2008).
6. S. Randel, D. Pilori, S. Chandrasekhar, G. Raybon, and P.J. Winzer "100-Gb/s Discrete-Multitone Transmission Over 80-km SSMF Using Single-Sideband Modulation With Novel Interference-Cancellation Scheme," Proc. of European Conference of Optical Communications 2015 (ECOC15), Valencia – Spain, Paper 0697 (2015).
7. H. Voelcker, "Demodulation of Single-Sideband Signals Via Envelope Detection," IEEE Trans. Comm. Technol. **14**, 22–30 (1966).

8. R. de L. Kronig "On the theory of the dispersion of X-rays," J. Opt. Soc. Am. **12**, 547–557 (1926).
9. H.A. Kramers, "La diffusion de la lumiere par les atomes," Atti Cong. Intern. Fisici, Como – Italy, Transactions of Volta Centenary Congress **2**, 545–557 (1927).
10. M. Cini, "The Response Characteristics of Linear Systems," J. Appl. Phys. **21**, 8–10 (1950).
11. M. Gell-Mann and M.L. Goldberger, "The formal theory of scattering," Phys. Rev. **91**, 398–408 (1953).
12. W. Heisenberg, "Quantum Theory of Fields and Elementary Particles," Rev. Mod. Phys. **29**, 269–278 (1957).
13. A. Mecozzi, "Retrieving the full optical response from amplitude data by Hilbert transform," Optics Comm. **282** 4183–4187 (2009).
14. A. Mecozzi, "A necessary and sufficient condition for minimum phase and implications for phase retrieval," available at http://arxiv.org/abs/1606.04861
15. Y. Shechtman, Y. C. Eldar, O. Cohen, H. N. Chapman, J. Miao, and M. Segev, "Phase Retrieval with Application to Optical Imaging: A contemporary overview," IEEE Signal Processing Magazine **32**, 87–109 (2015).
16. H. W. Bode, "Network Analysis and Feedback Amplifier Design," Chapter 8, D. Van Nostrand Co. Inc., 250 Fourth Ave., NewYork (1945).
17. A. V. Oppenheim, R. W. Schafer, and J.R. Buck, *Discrete-time signal processing*, Upper Saddle River, N.J., Prentice Hall, 1999, ISBN 0-13-754920-2.